A model for hydrogen detonation diffraction or transmission to a non-confined layer

Radulescu, M.I.[1], Mével, R.[2], Xiao, Q.[3] and Gallier, S.[4]

[1] *Department of Mechanical Engineering, University of Ottawa, Ottawa (ON) K1N 6N5 Canada, matei@uottawa.ca*

[2] *Center for Combustion Energy, School of Vehicle and Mobility, Tsinghua University, Beijing, China, mevel@mail.tsinghua.edu.cn*

[3] *National Key Laboratory of Transient Physics, Nanjing University of Science and Technology, Nanjing, 210094, China, qxiao@njust.edu.cn*

[4] *ArianeGroup, Le Bouchet Research Center, 91710 Vert le Petit, France, stany.gallier@ariane.group*

ABSTRACT

One strategy for arresting propagating detonation waves in pipes is by imposing a sudden area enlargement, which provides a rapid lateral divergence of the gases in the reaction zone and attenuates the leading shock. For sufficiently small tube diameter, the detonation decays to a deflagration and the shock decays to negligible strengths. This is known as the *critical tube diameter* problem. In the present study, we provide a closed form model to predict the detonation quenching for 2D channels. This problem also applies to the transmission of a detonation wave from a confined layer to a weakly-confined layer. Whitham's geometric shock dynamics, coupled with a shock evolution law based on shocks sustained by a constant source obtained by the shock change equations of Radulescu, is shown to capture the lateral shock dynamics response to the failure wave originating at the expansion corner. A criterion for successful detonation transmission to open space is that the lateral strain rate provided by the failure wave not exceed the critical strain rate of steady curved detonations. Using the critical lateral strain rate obtained by He and Clavin, a closed form solution is obtained for the critical channel opening permitting detonation transmission. The predicted critical channel width is found in excellent agreement with our recent experiments and simulations of diffracting $H_2/O_2/Ar$ detonations. Model comparison with available data for H_2/air detonation diffraction into open space at ambient conditions, or for transmission into a weakly confined layer by air is also found in good agreement, within a factor never exceeding 2 for the critical opening or layer dimension.

1.0 INTRODUCTION

When a detonation wave emerges from a tube or channel into an open space, the sudden expansion of the gases in the reaction zone of the detonation wave weakens the front. If the opening is sufficiently small, or the transmission is into a sufficiently thin non-confined layer, the detonation can degenerate into a weak shock followed by a deflagration wave. This so-called critical tube diameter problem, or critical channel height in 2D, has attracted much interest since the pioneering work of Zel'dovich et al. [1], due to its practical importance in detonation initiation or quenching applications. A review of the state of the art can be found in the PhD thesis of Schultz [2]. In spite of numerous efforts in modeling the diffraction process, a predictive model for the critical tube diameter is still lacking [3]. This is due in part to the presence of a cellular structure of the front of all detonations, which modifies the reaction zone structure of detonations and its sensitivity to the global expansion during the diffraction process. Nevertheless, recent work by Xiao et al. in slowly enlarging channels has shown that the quasi-steady dynamics of hydrogen detonations at low pressure, which are characterized by much longer reaction zones as compared to induction zones, can be well captured by the predictions of the ZND model with curvature [4]. It is thus of interest to verify whether the diffraction process can be equally well predicted by neglecting the influence of the cellular structure in hydrogen detonations.

The prediction of the diffraction process requires modeling the dynamics of diffracting detonations and

the distribution of transverse flow strain rate (i.e., curvature times flow speed) behind the lead shock. Previous studies have shown that the reaction zone decouples from the lead shock behind a failure wave propagating to the axis [5]. The shape of the shock wave was shown to be approximately self-similar by Bartlma and Schroder [6], and approximately captured by Whitham's geometrical shock dynamics theory for inert shock waves [7]. Arienti compared the curvature predicted by the model of Whitham with his computations and found it under-predicted the wave curvature [8]. Wescott, Stewart and Bdzil (henceforth WSB) have extended Whitham's characteristic rule to under-driven detonation waves by assuming quasi-steady dynamics and a reaction zone with an embedded sonic surface, but did not compare their predictions to gaseous diffracting detonations with sensible shock sensitivity permitting local extinction [9]. Recently, Mevel, Xiao and Radulescu have conducted detailed numerical simulations and experiments of diffracting detonations in $2H_2+O_2+2Ar$ [10]. In this study, we wish to compare the predictions of Whitham and WSB curvature distribution behind the diffracting detonation waves with our recent experiments and simulations.

While both Whitham's and the WSB models will be shown to provide an adequate approximation for the lateral strain rate distribution required for predicting failure, we also introduce a novel self-similar approximation for the shock dynamics weakly sustained by a rear piston, mimicking the weak support of the shock by the reaction products of a failed detonation wave. This model provides an improved prediction for the detonation dynamics. Combining the prediction of lateral strain rate and the maximum strain rate obtained for steady waves [11–13], we obtain a closed form expression for the critical channel height for detonation transmission. We show that the closed form prediction for detonation failure is in very good agreement with both the experiments and simulations.

The paper is organized as follows. We first briefly review our previous numerical results and experiments. We then compare the detonation dynamics with the predictions of Whitham's Geometrical Shock Dynamics using the Whitham and Westcott's truncations utilizing the characteristic rule, as well as our sustained shock model. We conclude by formulating the critical diffraction model based on a maximum curvature and its comparison with experiment and simulations.

2.0 NUMERICS AND EXPERIMENTS

Our recent detonation diffraction experiments and simulations in $2H_2+O_2+2Ar$ are discussed in detail elsewhere [10]. Figure 1 shows three examples of supercritical, critical and subcritical diffraction obtained in the numerics using realistic chemical kinetics. For a fixed geometry, at a sufficiently low pressure and long reaction zone (row a), the detonation wave is quenched by a lateral failure wave originating at the corner, which penetrates to the axis of symmetry. The shock and reaction zone de-couple and decay. This is the classical failure dynamics observed in the past experiments and simulations with realistic parameters of gas phase detonations. At a sufficiently high pressure and short reaction zone (row c), the failure wave cannot penetrate to the axis and the detonation wave never extinguishes on the axis. Instead, it continues to propagate with a cellular structure. At critical conditions intermediate to the two others (row b in the figure), re-inititiation is observed through the amplification of transverse waves, previously discussed in detail by Arienti and Shepherd [5, 8].

The experiments showed very similar dynamics. Close to the limit, the failure wave does not penetrate to the axis and a curved detonation wave survives quenching (Fig. 2). At the limit (Fig. 3), re-initiation occurs from a transverse wave amplification into a transverse detonation wave. The origin of this surviving triple point can be traced back to the axis in subfigure a), which also coincides closely to the failure wave arrival at the top wall. In this sense, this critical experiment offers a magnifying glass on the critical dynamics of diffraction. The detonation wave survives quenching at the axis by the amplification of transverse modes.

Table 1 provides a summary of the limits observed experimentally and numerically in terms of the ratio

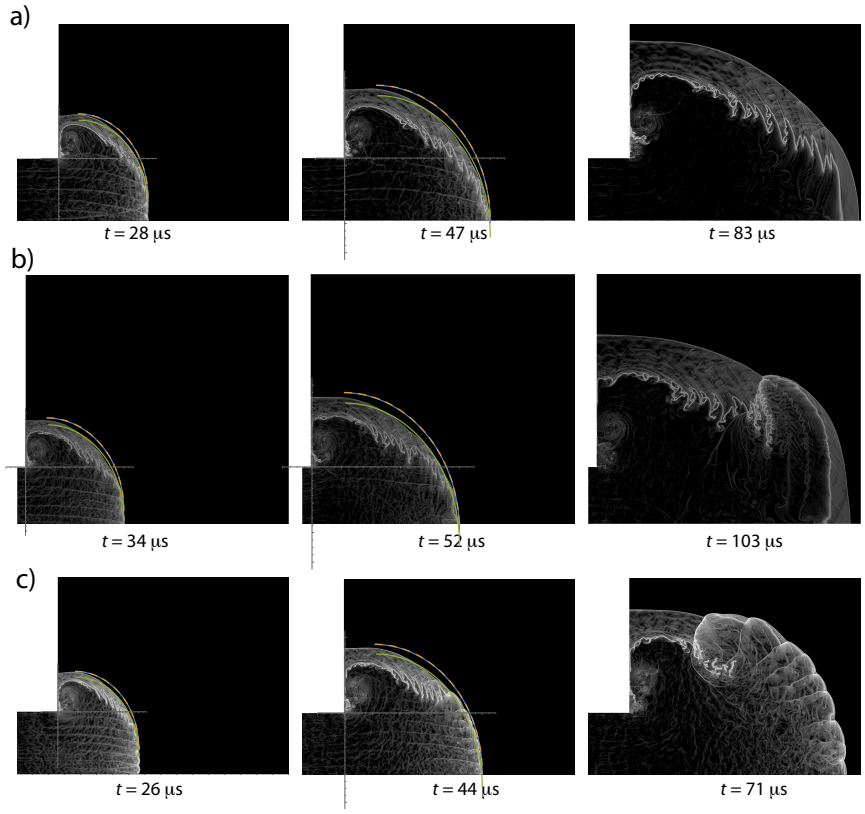

Figure 1: Numerical schlieren images adapted from [10] of diffracting detonations in a $2H_2$+O_2+2Ar mixture at $T_0 = 295$K; a) subcritical diffraction, $p_0 = 6.9$kPa, b) critical diffraction, $p_0 = 10.3$kPa; c) supercritical diffraction $p_0 = 13.8$kPa; the height of the computational domain is 188 mm; the time indicated below the images corresponds to the time after the detonation exits the channel; overlaid curves are for a weakly supported shock (green), Whitham's inert shock model (orange) and WSB model (blue).

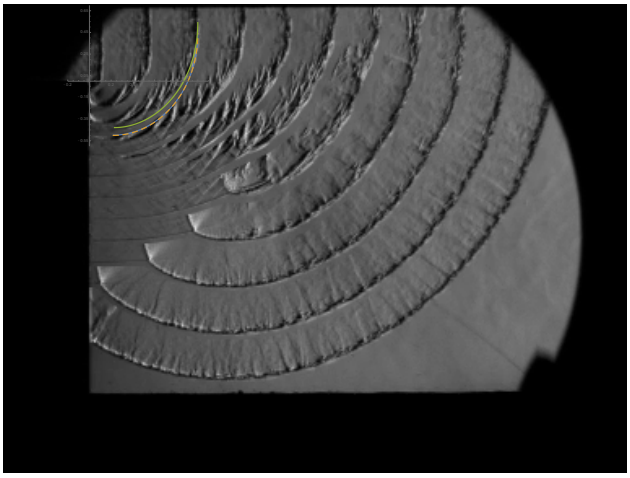

Figure 2: Composite schlieren images of detonation diffraction in $2H_2$+O_2+2Ar mixture at $T_0 = 295$K and $p_0 = 23$kPa, adapted from [10]; the distance between the bottom and top walls is 200 mm; overlaid curves are for a weakly supported shock (green), Whitham's inert shock model (orange) and the WSB model (blue).

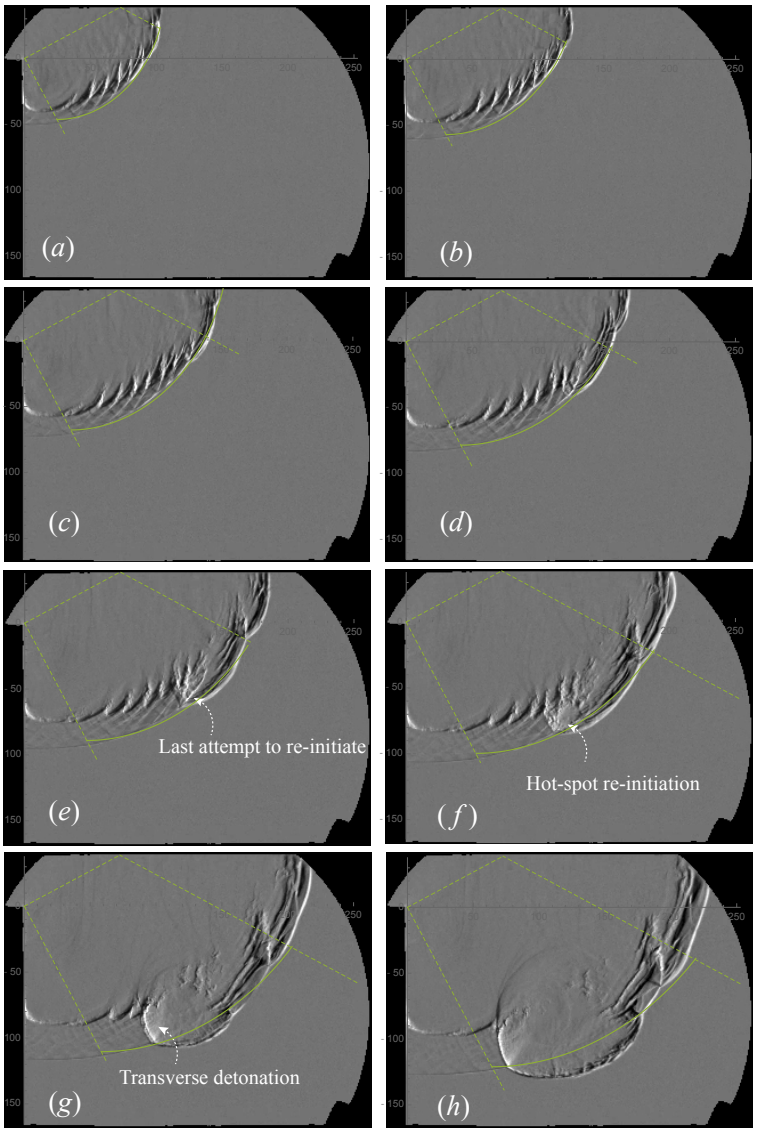

Figure 3: Composite schlieren images of detonation diffraction in $2H_2+O_2+2Ar$ mixture at $T_0 = 295$K and $p_0 = 17$kPa, adapted from [10]; the distance between the bottom and top walls is 200 mm; overlaid in green is the shock shape predicted with the weakly supported shock assumption.

between the channel bi-thickness W normalized by the ZND induction zone length. For reducing the experiments, since the detonation prior to diffraction was found to propagate at a speed lower than CJ due to wall losses, the channel width was normalized by the induction zone length calculated for the conditions of the weaker lead shock. The numerical limit of $W_\star/\Delta_i = 176$ was found approximately 30% lower than the experiments, where $W_\star/\Delta_i$ varied between 200 and 260. This variability in the experiments is due to the stochasticity, which can be attributed to the cellular structure controlling the details of the limiting phenomena, as illustrated in Fig. 3, for example.

Table 1: Summary of diffraction experiments and model prediction.

	n in (1)	n for $\gamma = 1.4$	$W_\star/\Delta_i$ (model)	$W_\star/\Delta_i$ (num)	$W_\star/\Delta_i$ (exp)
Whitham	$n_W = 1 + \frac{2}{\gamma} + \sqrt{\frac{2\gamma}{\gamma-1}}$	5.07	146	176	200-260
WSB	$n_{WBS} = 3\left(\frac{\gamma+1}{\gamma}\right)$	5.14	145	176	200-260
shock support	$n_R = 2\left(\frac{\gamma+1}{\gamma}\right)$	3.43	164	176	200-260

3.0 WHITHAM'S SELF-SIMILAR GSD SOLUTION FOR THE SHOCK CURVATURE DISTRIBUTION

Whitham's geometric shock dynamics (GSD) provides a simple framework to predict the dynamics of shocks affected by changes in the shock inclination angles, such as diffraction, as well as determine the curvature evolution [7]. For generic shock evolution equations of the form

$$\frac{S_w^2 \kappa}{\dot{S}_w} \equiv \frac{\mathrm{d}\ln A/\mathrm{d}x}{\mathrm{d}\ln S_w/\mathrm{d}x} = -n \tag{1}$$

(i.e., $S_w \propto A^{-1/n}$) where S_w is the normal speed of the shock with respect to a medium at rest, $\kappa = \frac{\mathrm{d}\ln A}{\mathrm{d}x}$ its local curvature, A a measure of the surface area of a shock element and n an arbitrary exponent, the shape of a diffracting shock over a sharp corner is given by equations (8.95) in Whitham [7]:

$$\frac{X}{S_w t} = \sqrt{\frac{n+1}{n}} \exp\left(\frac{\theta}{\sqrt{n}}\right) \sin\left(\eta - \theta\right) \tag{2}$$

$$\frac{Y}{S_w t} = \sqrt{\frac{n+1}{n}} \exp\left(\frac{\theta}{\sqrt{n}}\right) \cos\left(\eta - \theta\right) \tag{3}$$

where η is given by $\tan\eta = \sqrt{n}$ and θ is the angle of the unit normal to the shock surface with the x-axis, see Fig. 4. These expressions derive from a purely geometric theory for how surfaces given by a law like (1) evolve in space. The physics are reflected by the exponent n, which we treat below.

Since the shock surface is parameterized by θ in the form $\Lambda\left(X(\theta,t), Y(\theta,t)\right)$, its local curvature at a given time t is given by

$$\kappa = \frac{X_\theta Y_{\theta\theta} - Y_\theta X_{\theta\theta}}{\left(X_\theta^2 + Y_\theta^2\right)^{\frac{3}{2}}} \tag{4}$$

yielding

$$\kappa = \frac{1}{S_w t}\left(\frac{n}{n+1}\right) \exp\left(-\frac{\theta}{\sqrt{n}}\right) \tag{5}$$

The curvature thus decays with time and with increasing θ. The maximum curvature occurs for $\theta = 0$:

$$\kappa_0 = \frac{1}{S_w t}\left(\frac{n}{n+1}\right) \tag{6}$$

Adapting these results for our diffraction problem (see Fig. 5), where the half width of the channel is $W/2$, the time required for a transverse signal along the shock to reach $y = W/2$ is $\frac{1}{S_w}\frac{W}{2}\sqrt{n}$. At this time, the shock curvature given by (6) becomes

$$\kappa_0 = \frac{2}{W}\left(\frac{\sqrt{n}}{n+1}\right) \tag{7}$$

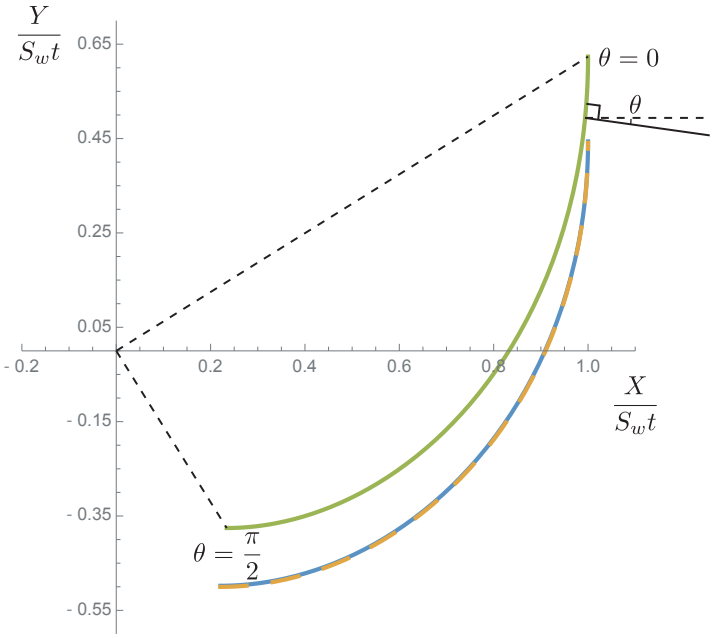

Figure 4: The self-similar solution predicted by GSD for $\gamma = 1.4$: weakly supported shock (green), Whitham's inert shock model (orange) and WSB model (blue).

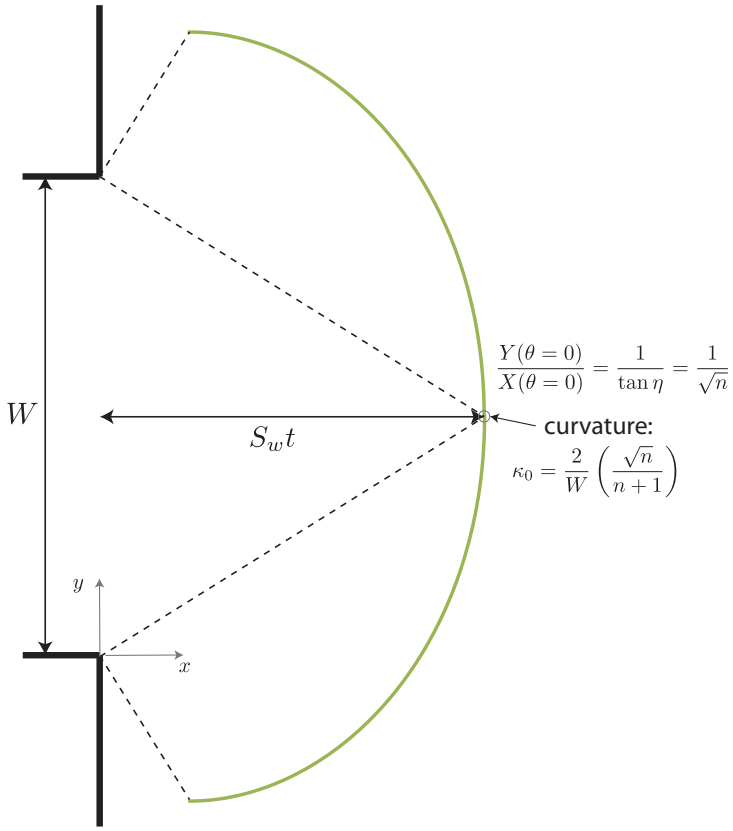

Figure 5: The GSD construction for approximating the shock shape when the corner signals meet.

4.0 CRITERION FOR DETONATION SUSTENANCE

For the detonation to survive quenching, the criterion we propose, compatible with our experiments and simulations, is that the maximum curvature of the wave given by (7) not exceed the critical curvature permitting steady curved detonations. The analytical work of He and Clavin [11], Yao and Stewart [13, 14] and Klein et al. [12] permits to express this critical curvature in closed form. We use the expression of critical curvature obtained by He and Clavin, which was found in very good agreement with realistic chemistry calculations [15]:

$$\kappa_\star^{-1} = \Delta_i \frac{8\mathrm{e}}{1-\gamma^{-2}} \left(\frac{E_a}{RT_N} \right) \tag{8}$$

where Δ_i is the induction zone length of the CJ detonation, T_N is the temperature behind the shock of the CJ detonation and $\frac{E_a}{RT_N}$ is the non-dimensional activation energy characterizing the sensitivity of the induction time to temperature. From (7), we obtain the critical channel height for successful detonation diffraction:

$$\frac{W_\star}{\Delta_i} = \frac{2\sqrt{n}}{n+1} \frac{8\mathrm{e}}{1-\gamma^{-2}} \left(\frac{E_a}{RT_N} \right) \tag{9}$$

The exponent n depends on the model of shock evolution adopted, as we will see next.

5.0 THE EXPONENT n FROM SHOCK EVOLUTION EQUATIONS

An exact solution for decaying shock waves yielding the exponent n is not currently available. Physically based approximations have been proposed, and we briefly review those relevant for the present problem of diffraction. Whitham's model for the shock evolution equation is obtained by projecting the shock state changes along the trajectory of a $C+$ characteristic. This model applies to shock waves for which the rear boundary conditions play a negligible influence on the shock dynamics. For strong shocks, Whitham [7] obtains the exponent n given by:

$$n = n_W = 1 + \frac{2}{\gamma} + \sqrt{\frac{2\gamma}{\gamma - 1}} \tag{10}$$

For $\gamma = 1.4$, corresponding to the post shock state in the experiments and numerics discussed above, this exponent is 5.07. The predictions of the decoupled detonation are shown in the Figs. 1, 2 and 3 as the orange curves. The model is in fair agreement with the experiments and numerics. Note that the Whitham exponent is sometimes erroneously quoted with $+$ in the square root instead of the $-$. This unfortunate typographical error in Bartlma and Schroder [6] has persisted in the more modern literature [16]. Using the incorrect exponent leads to better agreement with simulations and experiments, but a purely fortuitous one.

The characteristic rule has also been applied to underdriven detonations relevant to diffraction problems by Wescott et al. [9]. Their model assumes the detonation in quasi-steady state, and requires an embedded sonic surface. The resulting exponent n of their model for sonic under-driven detonations is:

$$n = n_{WBS} = 3 \left(\frac{\gamma + 1}{\gamma} \right) \tag{11}$$

The model reproduces one of the limits obtained by more rigorous perturbation methods by Yao and Stewart[14]. Again, this exponent has unfortunately also been reported erroneously (as the inverse of this expression above) in the paper of Wescott et al. For $\gamma = 1.4$, corresponding to the post shock state

in the experiments and numerics discussed above, the correct exponent is 5.14, i.e., almost identical to the inert shock model of Whitham. The shock prediction using this model is shown in blue; it provides the same fair agreement as the Whitham model for this value of γ, although they model fundamentally different phenomena.

The characteristic rule adopted in the previous two models is aimed to model the dynamics of shock waves not influenced by rear boundary conditions. This is physically inconsistent with the dynamics observed in experiments. For the detonation diffraction problem, the arrival of the failure wave quenches the chemical reactions by sudden flow expansion. The shock is subsequently partially supported by the motion of the products, which act as a piston and influence the shock dynamics, at least in the region immediately adjacent to the arrival of the failure wave and conducive to reaction quenching. This situation was analyzed for pulsed sources by Chekmarev [17] and Radulescu and Law [18] in the context of jets issuing from finite sized sources. These authors have found two asymptotic behaviors, the near field dynamics of the shock were controlled by the source outflow speed, while the far field was controlled by the free dynamics of the mass layer bounded by inner and outer facing shocks. The early dynamics of the failed detonation fronts can be argued to correspond to the former class. In the detonation problem, a rear facing shock is not formed, while for the diffraction of a purely inert shock, the rear facing shock is formed to match the post shock state to the supersonic expansion. Indeed, the flow in the lab frame following a detonation is subsonic, whereas it is supersonic for a strong inert shock. Based on these physical considerations, a physical model for shock dynamics in supported shocks is to assume that there is no time variation in the piston support, mimicking a constant rear support.

Radulescu has recently derived an exact expression linking $\frac{\partial u}{\partial t}$ with the dynamics of curved shocks using Fickett and Davis' shock change equations [19]. For strong inert shocks,

$$\frac{(\gamma+1)^2}{4\gamma}\frac{1}{\dot{S}_w}\frac{\partial u}{\partial t} = 2\left(\frac{\gamma+1}{\gamma}\right) + \frac{S_w^2\kappa}{\dot{S}_w} \tag{12}$$

For a quasi-steady rear support, we neglect the variation of the rear support compared with the shock speed variation, i.e., neglect the LHS. This leads to a simple evolution equation for the shock of the desired form (1), with n given by

$$n = n_R = 2\left(\frac{\gamma+1}{\gamma}\right) \tag{13}$$

For $\gamma = 1.4$, corresponding to the post shock state in the experiments and numerics discussed above, this exponent is 3.43. The shock dynamics predicted by this truncation for the shock dynamics are shown in green in Figs. 1, 2 and 3. The simple model is found in excellent agreement with simulations and experiment. It can thus serve to evaluate the lateral strain rate behind the shock when the failure wave reaches the axis, as discussed above.

To further illustrate however how the detonation diffraction problem differs from the problem of diffraction of an inert shock, we have computed numerically the diffraction of a Mach $M = 5$ shock for $\gamma = 1.4$, the same parameters as for the reactive case. The self-similar density field is shown in Fig. 6, along with the predictions of shock dynamics discussed above. Clearly, for the inert shock dynamics, the shock shape is well captured by the Whitham characteristic rule. Note however the barrel shock system that separates the supersonic steady expansion of the flow passing the corner and the gas layered between the inner and outer facing shocks, whose dynamics dictate the shock evolution. This is fundamentally different from the detonation diffraction process, where these elements are absent and are replaced by a wall vortex.

The discussion of the shock dynamics predicted by different physics has shown that the shape of the diffracting shock is weakly dependent on which model is used. More fundamentally, while the diffraction process is not expected to be strictly self-similar, as the local front is more likely well approximated by

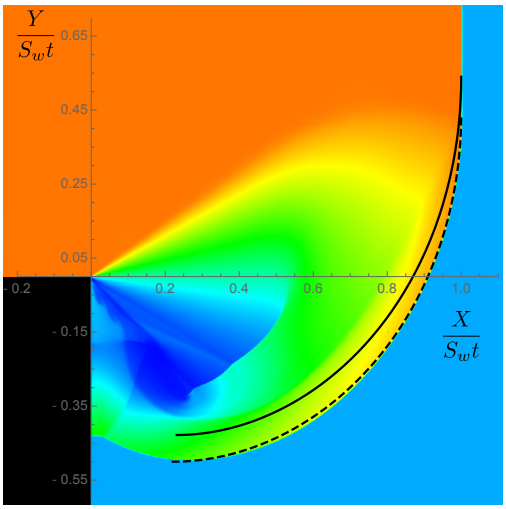

Figure 6: The density distribution during the diffraction of a $M_w = 5$ and $\gamma = 1.4$ inert shock at a $\pi/2$ corner; overlaid curves are for a weakly supported shock (solid line) and Whitham's inert shock model obtained with the characteristic rule.

the WSB model close to the axis where the reactions are still coupled, our model when reactions fail and the shock is piston-supported and the Whitham inert model further from the axis, the close coincidence of these exponents suggests quasi-self similarity. For engineering purposes, taking any of them should be satisfactory. Nevertheless, a formal multi-scale analysis is warranted in the framework of Bdzil and Stewart's Detonation Shock Dynamics [20] formulated for a kinetic law compatible with the long reaction zone character of hydrogen detonations. This is well outside the scope of the present discussion, which aims at formulating an approximate transmission criterion.

6.0 TRANSMISSION CRITERION

With the exponent n in closed form from the different approximations discussed above, the critical channel height for detonation transmission to open space can be obtained in closed form by substituting the expressions for n given above in (9). For our model with quasi-constant rear support, we obtain:

$$\frac{W_\star}{\Delta_i} = \frac{16\sqrt{2}\mathrm{e}\sqrt{\gamma^5(\gamma+1)}}{(2+3\gamma)(\gamma^2-1)}\left(\frac{E_a}{RT_N}\right) \tag{14}$$

Similar expressions can be obtained using the other expressions for the constant n. For the $2H_2+O_2+2Ar$ mixture tested, the postshock γ is 1.4 and the reduced activation energy is 4.4, obtained from the sensitivity of the ignition delay to temperature changes at the Von Neuman state using Cantera for the calculations. The resulting predictions of critical channel width using the different values of n are shown in Table 1, along with the experimental and numerical values obtained in our previous experiments and simulations discussed above. The weakly supported shock model predicts the critical value obtained from the simulations with an error of less than 7%. The predictions based on Whitham and Westcott et al. models for the shock dynamics underestimate the critical channel width by 17%, which is also quite remarkable. All the models underpredict the experiment, for which the limit is approximately 30% larger than for the numerics.

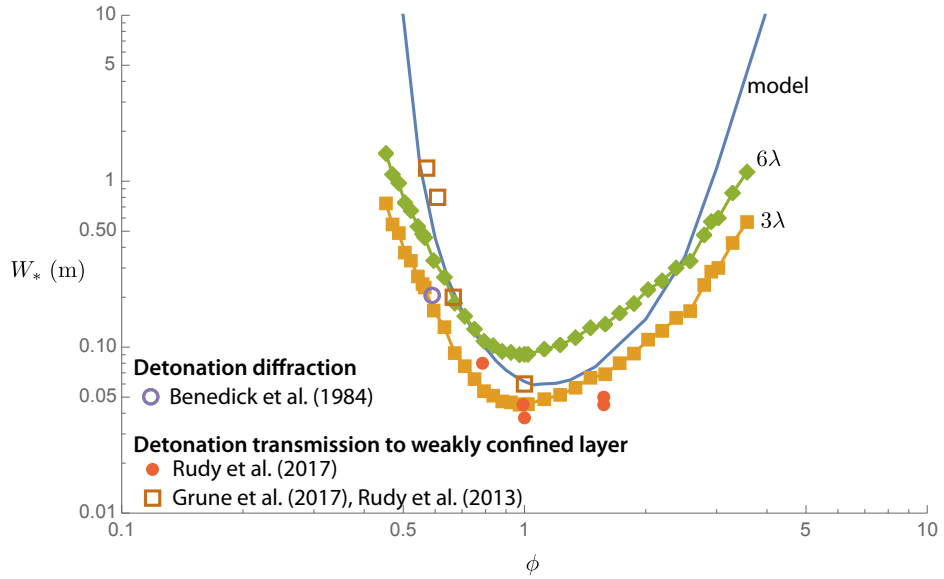

Figure 7: The critical channel height for H_2/air detonation transmission to open space at ambient conditions in terms of the fuel-air equivalence ratio; connected symbols are cell size correlations using the data of Guirao et al. [23]; symbols are experiments for detonation transmission to open space of Benedick et al. [22] and for detonation transmission into a weakly confined layer of Rudy, Grune and their co-workers [24–26]; data reported for layers of width $W/2$ confined on a single side are reported in terms of the bi-thickness W.

7.0 TRANSMISSION AND PROPAGATION IN H_2-AIR MIXTURES

The model formulated was found in very good agreement with our laboratory experiments and numerical simulations in the low-pressure $2H_2+O_2+2Ar$ mixture tested. It is worthwhile nonetheless to test its predictive capability for H_2/air mixtures at ambient conditions of 1 atmosphere and 298 K. Fig. 7 reports the resulting critical channel thickness $W_\star$ at different fuel-air equivalence ratios. In evaluating $W_\star$ from (14), the induction zone length was evaluated using an in-house ZND code [21] and the activation energy was evaluated by computing the derivative of the logarithm of the ignition delay computed at constant volume with the inverse initial temperature at the Von Neumann condition behind a shock propagating at the Chapman-Jouguet velocity [21]. The ratio of specific heats was also evaluated at the Von Neumann condition. The kinetic calculations were performed using the San Diego 2016 chemical kinetic mechanism. The results of the model proposed are compared with the experimental value determined by Benedick et al. in large scale field trials detonation diffraction experiments [22]. Also shown are the results of detonation transmission from a confined layer to a layer weakly confined by inert gas obtained by Rudy, Grune and their co-workers. While the transmission from a confined to a non-confined layer is not exactly the same problem as the one modeled, it is expected to be very similar, since the transmission is controlled by the side rarefactions penetrating to the axis. Transmission into the layer by preventing quenching is a necessary and sufficient condition for subsequent steady propagation. While there is some scatter in the experimental data by approximately a factor of 2, our model captures the experimental results surprisingly well, within this scatter.

Also shown in Fig. 7 is the correlation proposed by Benedick et al. $W_\star \simeq 3\lambda$, where λ is the detonation cell size; we also show the same data with $W_\star \simeq 6\lambda$ to illustrate the factor of 2 difference. We used the cell size data reported by Guirao et al. [23], on which this correlation was first developed. Note that Grune et al. and Rudy et al. propose $W_\star \simeq 6\lambda$, although they use a different data set for cell sizes. While

these correlations are in good agreement with the experimental data near stoichiometric conditions, some departures are evident in lean mixtures, for which our model works very well.

It thus appears that the closed form model derived works equally well for H_2/air mixtures at ambient conditions and accurately predict, by a factor never exceeding 2, the critical channel dimension or opening height that will transmit a detonation into free space, or space confined only on one side.

8.0 CONCLUSIONS

The proposed model for critical detonation diffraction relies on the prediction of the wave curvature effected by the failure wave originating from the diffraction corner. While the models of Whitham and Westcott, Bdzil and Stewart are found to predict these dynamics fairly well, we propose an improvement on the shock dynamic prediction using a weakly supported shock model, which is found in excellent agreement with experiment and simulations. Using these simple estimates for the maximum wave curvature attained when the failure waves meet the axis, a simple criterion for successful transmission is that this curvature not exceed the maximum curvature that can be sustained by a curved detonation in quasi-steady state. The closed form limits obtained for the critical diffraction channel height are found in excellent agreement with numerics and under-predict the experiments by approximately 40% in the low-pressure $2H_2+O_2+2Ar$. Model comparison with available data of H_2/air detonation diffraction into open space at ambient conditions, or for transmission into a weakly confined layer by air is also found in good agreement, within a factor never exceeding 2.

1. Zel'dovich, I.B., Kogarko, S.M. and Simonov, N.N., An experimental investigation of spherical detonation, *Soviet Physics-Technical Physics*, **1**, no. 8, (1956), pp. 1689–1713.
2. Schultz, E., Detonation diffraction through an abrupt area expansion, Ph.D. thesis, California Institute of Technology, Pasadena, California, 2000.
3. Lee, J.H.S., Dynamic parameters of gaseous detonations, *Annual Review of Fluid Mechanics*, **16**, (1984), pp. 311–336.
4. Xiao, Q. and Radulescu, M.I., Dynamics of hydrogen-oxygen-argon cellular detonations with a constant mean lateral strain rate, *Combustion and Flame*, **215**, (2020), pp. 437–457.
5. Arienti, M. and Shepherd, J.E., A numerical study of detonation diffraction, *Journal of Fluid Mechanics*, **529**, (2005), pp. 117–146.
6. Bartlma, F. and Schroder, K., The diffraction of a plane detonation wave at a convex corner, *Combustion and Flame*, **66**, no. 3, (1986), pp. 237–248.
7. Whitham, G.B., Linear and nonlinear waves, Wiley, New York, 1974.
8. Arienti, M., A numerical and analytical study of detonation diffraction, Ph.D. thesis, California Institute of Technology, Pasadena, California, 2003.
9. Wescott, B.L., Stewart, D.S. and Bdzil, J.B., On self-similarity of detonation diffraction, *Physics of Fluids*, **16**, no. 2, (2004), pp. 373–384.
10. Mevel, R., Xiao, Q. and Radulescu, M.I., Hydrogen-oxygen-argon detonation diffraction in a narrow channel, Proceedings of the 26th International Colloquium on Dynamics of Explosions and Reactive Systems, Boston, MA, p. 6.
11. He, L. and Clavin, P., On the direct initiation of gaseous detonations by an energy source, *Journal of fluid mechanics*, **277**, (1994), pp. 227–248.
12. Klein, R., Krok, J.C. and Shepherd, J.E., Curved quasi-steady detonations: Asymptotic analysis and detailed chemical kinetics, Technical report, California Institute of Technology, Pasadena, California, 1995, GALCIT Report FM 95-04.

13. Yao, J. and Stewart, D.S., On the normal detonation shock velocity - curvature relationship for materials with large activation energy, *Combustion and Flame*, **100**, no. 4, (1995), pp. 519–528.
14. Yao, J. and Stewart, D.S., On the dynamics of multi-dimensional detonation, *Journal of Fluid Mechanics*, **309**, (1996), pp. 225–275.
15. Radulescu, M.I. and Lee, J.H., The failure mechanism of gaseous detonations: experiments in porous wall tubes, *Combustion and Flame*, **131**, no. 1-2, (2002), pp. 29–46.
16. Yuan, X.Q., Mi, X.C., Ng, H.D. and Zhou, J., A model for the trajectory of the transverse detonation resulting from re-initiation of a diffracted detonation, *Shock Waves*, **30**, no. 1, (2020), pp. 13–27.
17. Chekmarev, S.F., Nonsteady radial expansion of a gas into a flooded space from a suddenly turned on steady source, *Journal of Applied Mechanics and Technical Physics*, **16**, no. 2, (1975), pp. 209–216.
18. Radulescu, M.I. and Law, C.K., The transient start of supersonic jets, *Journal of Fluid Mechanics*, **578**, (2007), pp. 331–369.
19. Radulescu, M.I., On the shock change equations, *Physics of Fluids*, **32**, no. 5, (2020), p. 056106.
20. Bdzil, J.B. and Stewart, D.S., Time-dependent two-dimensional detonation: the interaction of edge rarefactions with finite-length reaction zones, *Journal of Fluid Mechanics*, **171**, (1986), pp. 1–26.
21. Radulescu, M.I. and Borzou, B., Dynamics of detonations with a constant mean flow divergence, *Journal of Fluid Mechanics*, **845**, (2018), pp. 346–377.
22. Benedick, W.B., Knystautas, R. and Lee, J.H., Dynamics of Shock Waves, Explosions and Detonations, American Institute of Aeronautics and Astronautics, *Progress in Astronautics and Aereonautics*, volume 94, chapter Large-Scale Experiments on the Transmission of Fuel-Air Detonations from two-dimensional channels, 1984, pp. 546–555.
23. Guirao, C., Knystautas, R., Lee, J., Benedick, W. and Berman, M., Hydrogen-air detonations, Nineteenth Symposium (International) on Combustion/The Combustion Institute, pp. 583–590.
24. Rudy, W., Kuznetsov, M., Porowski, R., Teodorczyk, A., Grune, J. and Sempert, K., Critical conditions of hydrogen-air detonation in partially confined geometry, *Proceedings of the Combustion Institute*, **34**, no. 2, (2013), pp. 1965–1972.
25. Grune, J., Sempert, K., Friedrich, A., Kuznetsov, M. and Jordan, T., Detonation wave propagation in semi-confined layers of hydrogen-air and hydrogen-oxygen mixtures, *International Journal of Hydrogen Energy*, **42**, no. 11, (2017), pp. 7589–7599.
26. Rudy, W., Dziubanii, K., Zbikowski, M. and Teodorczyk, A., Experimental determination of critical conditions for hydrogen-air detonation propagation in partially confined geometry, *International Journal of Hydrogen Energy*, **42**, no. 11, (2017), pp. 7366–7373.